Breakdown of Temporal Coherence in Photon Condensates

Yijun Tang,[1] Himadri S. Dhar,[2] Rupert F. Oulton,[1] Robert A. Nyman,[1] and Florian Mintert[1,3]
[1]*Physics Department, Blackett Laboratory, Imperial College London, Prince Consort Road, SW7 2AZ, United Kingdom*
[2]*Department of Physics, Indian Institute of Technology Bombay, Powai, Mumbai 400076, India*
[3]*Helmholtz-Zentrum Dresden-Rossendorf, Bautzner Landstraße 400, 01328 Dresden, Germany*

(Received 25 October 2023; accepted 20 March 2024; published 23 April 2024)

The temporal coherence of an ideal Bose gas increases as the system approaches the Bose-Einstein condensation threshold from below, with coherence time diverging at the critical point. However, counterexamples have been observed for condensates of photons formed in an externally pumped, dye-filled microcavity, wherein the coherence time decreases rapidly for increasing particle number above threshold. This Letter establishes intermode correlations as the central explanation for the experimentally observed dramatic decrease in the coherence time beyond critical pump power.

DOI: 10.1103/PhysRevLett.132.173601

Coherence is a ubiquitous feature of wave mechanics that plays an important role in various fields of science, ranging from quantum computing [1] to electronic coherence [2] and neurobiology [3]. Originally the notion of coherence had mostly been discussed in experiments involving light [4], but since the development of quantum theory, spatial and temporal coherence can also be observed in massive particles with particularly pronounced wavelike behavior, such as Bose-Einstein condensates (BEC) [5].

While lasers are the best known sources of coherent light [4], unlike matter waves or BECs, they primarily operate deep in the nonequilibrium regime. However, in recent years, photonic systems such as polaritons and photons in a microcavity and excitons in semiconductors, have been curated to undergo a phase transition that spontaneously creates a spatiotemporal coherent light similar to an atomic BEC [6–10]. While still driven dissipative in nature, in contrast to lasers, these systems operate in a quasiequilibrium regime and offer rich dynamics and coherent phenomena [11], ranging from simultaneous condensation in multiple modes [12], vortexlike structures [13], critical behavior [14], and particle correlation [15,16] in photons to superfluidity [17] and topological lasing [18] in polaritons.

Our work here focuses on the temporal coherence properties of Bose-Einstein condensates of photons, formed inside a dye-filled microcavity [7,8]. A defining characteristic of photon BECs is that thermalization is achieved not due to some intrinsic nonlinearity and particle interaction but rather through incoherent interactions between the photon gas and the dye molecules, driven by an incoherent pump [19,20]. Phase coherence in these condensates results from photon emission from molecules [21], and experimental observations show a spontaneous transition from short-range coherence at thermal scale to long-range coherence in the BEC phase [22,23].

The temporal coherence time τ of light inside the cavity is experimentally observed to grow with increasing photon number n as the system approaches the BEC threshold from below [22,23]. This is consistent with the well-known Schawlow-Townes limit $\tau \propto n$ for $n \gg 1$ [24]. A microscopic model of photon BEC in a single mode cavity, gives a closed theoretical expression for τ, which indeed reduces to the Schawlow-Townes limit for large n [25]. However, experimental observations show that this is no longer the case for high photon numbers beyond the transition threshold [12,22]. In contrast, the temporal coherence breaks down and the coherence time decreases dramatically as the pump power is increased above the BEC critical point.

Based on a concurrently developed framework for photon-photon correlations in driven-dissipative photon gases [26], we show that intermode correlations and competition of different photon modes for access to molecular excitations are the primary reason for the breakdown in temporal coherence, as experimentally observed in photon condensates inside a dye-filled microcavity [12,22].

A small decrease of molecular excitations can have a substantial impact on the photonic state inside the cavity, such as loss of population or decondensation of individual modes [27]. Intermode correlations, even if weak, can alter the molecular excitation profile, and we show that this can cause a loss of temporal coherence in the condensed mode without affecting the mode population. This allows the coherence time τ to decrease even when the mode population n is large, contradicting the Schawlow-Townes limit, as observed in experimental studies of temporal coherence in photonic BECs formed inside a dye-filled microcavity [12]. Moreover, this observation is larger than any loss of coherence that may arise from small nonlinear effects such as the Henry factor [28] or thermo-optical effects [29,30].

The temporal coherence between a pair of modes p and q of a photonic system can be characterized in terms of the two-time correlation function [4],

$$c_{pq}(t_2 - t_1) = \langle \hat{a}_p^\dagger(t_2)\hat{a}_q(t_1)\rangle, \tag{1}$$

where $\hat{a}_k(\hat{a}_k^\dagger)$ are the annihilation (creation) operator for the kth photon mode, which, in steady-state experiments, depends only on the time difference $t = t_2 - t_1$. The real and imaginary terms of the function $c_{pq}(t)$ can be directly measured in the ports of a delayed-arm optical interferometer [4]. To represent correlation functions for multiple modes in a compact form, we can consider the vectors $\mathbf{c}_p$ with elements $[\mathbf{c}_p]_q = c_{pq}e^{-i\omega_p t}$. Starting from a microscopic, mode-coupled model of photon condensation in a dye-filled microcavity [13,31], it is shown in Ref. [26] that the equation of motion for each of the correlation function vectors $\mathbf{c}_p$ is given by

$$\frac{d\mathbf{c}_p(t)}{dt} = -\frac{1}{2}\left(\kappa + \mathbf{A}\mathbf{h} - (\mathbf{A}+\mathbf{E})\mathbf{f}\right)\mathbf{c}_p(t), \tag{2}$$

where $\mathbf{A}$ and $\mathbf{E}$ are diagonal matrices with elements $\mathcal{A}_k$ and $\mathcal{E}_k$, which are the rates at which photons in mode k are absorbed and emitted by the dye molecules. The matrices $\mathbf{h}$ and $\mathbf{f}$ have elements

$$\mathbf{h}_{pq} = \int d\mu(\mathbf{r})\psi_p^*(\mathbf{r})\psi_q(\mathbf{r}), \quad \text{and} \tag{3}$$

$$\mathbf{f}_{pq} = \int d\mu(\mathbf{r})\psi_p^*(\mathbf{r})\psi_q(\mathbf{r})f(\mathbf{r}), \tag{4}$$

which are defined in terms of the Hermite-Gaussian mode functions $\psi_p(\mathbf{r})$ of the cavity, the molecular density $\mu(\mathbf{r})$ and the local excitation fraction $f(\mathbf{r})$ of the molecules, at position $\mathbf{r}$ in the cavity plane. The terms $\mathbf{h}_{pq}$ and $\mathbf{f}_{pq}$, represent the total and excited number of molecules, respectively, that can be simultaneously accessed by modes p and q, as governed by the overlap term $\psi_p^*(\mathbf{r})\psi_q(\mathbf{r})$. These values depend on the experimental setup of the dye-filled microcavity [22]. The lowest energy mode ω_0 depends on the cutoff frequency, which is set by cavity length and the mode spacing $\Delta\omega$ by the curvature of the mirror. The modes of the cavity are thus given by $\omega_k = \omega_0 + k\Delta\omega$, and the properties of the dye govern the rates of absorption $\mathcal{A}_k$ and emission $\mathcal{E}_k$. The choice of the cutoff frequency and the ensuing absorption-emission spectra is important to create near-equilibrium conditions that allow the photons to thermalize and condense [19,32]. The dye is incoherently excited with a pump rate $\Gamma_\uparrow$, which introduces photons inside the cavity via spontaneous and stimulated processes, while photons and molecules are lost with rates κ and $\Gamma_\downarrow$, respectively. The pump has a Gaussian profile, focused at the center of the cavity, with the molecular density $\mu(\mathbf{r})$ assumed to be uniform.

While $\psi_p(\mathbf{r})$, $\mu(\mathbf{r})$, κ, $\mathbf{E}$, $\mathbf{A}$, and $\mathbf{h}$ remain unchanged for a specific experimental setting, $\mathbf{f}$ is dependent on the excitation fraction $f(\mathbf{r})$, which is time dependent. However, for most experiments, the longtime, steady state of the system is often of primary interest, and this state will be taken as the initial state in the following discussion. Temporal changes in the excitation of the dye molecules are thus negligible. Now, the steady state values of $f(\mathbf{r})$ and the correlation function $\mathbf{c}_p(0)$ are obtained by solving the equations of motion of the microscopic model [13,31], where the term $n_p = c_{pp}(0)$ gives the population of mode p, and $n_{pq} = c_{pq}(0)$ is the intermode correlation between modes p and q. Importantly, the intermode correlations arise from terms such as $(\mathbf{A}+\mathbf{E})\mathbf{f}$, which allow for molecules at $\mathbf{r}$ to absorb excitation from mode p and emit to mode q based on the overlap of the mode functions and the excitation profile $\psi_p^*(\mathbf{r})\psi_q(\mathbf{r})f(\mathbf{r})$ [26].

Equation (2) indicates that in the absence of any dye inside the cavity the temporal coherence of each individual mode would simply decay on a timescale proportional to the photon loss rate κ. The presence of the dye inside the cavity and the ensuing absorption and emission of photons by the dye molecules give rise to additional terms. In particular, irrespective of the photonic state in the cavity, the absorption of photons by the molecules leads to an additional decay due to the term $\mathbf{A}\mathbf{h}$, which accelerates the decay of coherence. On the other hand, the temporal coherence in the system is boosted by the term $(\mathbf{A}+\mathbf{E})\mathbf{f}$, which is intuitively expected as the coherence increases as the molecular excitations increase and the photon gas in the cavity is driven towards the BEC phase transition. These general observations apply equally well to the case of single mode systems [25].

The sudden loss of temporal coherence can be seen in Fig. 1, that depicts the coherence time τ_p obtained from the solution $\tilde{\mathbf{c}}_p(t) = \exp[-t/\tau_p]\tilde{\mathbf{c}}_p(0)$ of Eq. (2) [13,31]. The figure shows the ground state coherence time τ_0 as a function of the pump rate $\Gamma_\uparrow$, both below and above the BEC threshold. The condensation of the ground state (mode [0]) leads to a sharp growth of the coherence time. Importantly, the coherence reaches its maximum around $1.18\Gamma_\downarrow$, at the point when the population of the second excited state (mode [2]) starts growing. A subsequent increase in $\Gamma_\uparrow$ leads to a sharp decline in the temporal coherence of the ground state and a decrease of τ_0, consistent with recent experimental observations [12].

A simple qualitative picture for the coherence time emerges if the matrices $\mathbf{h}$ and $\mathbf{f}$ can be considered to be

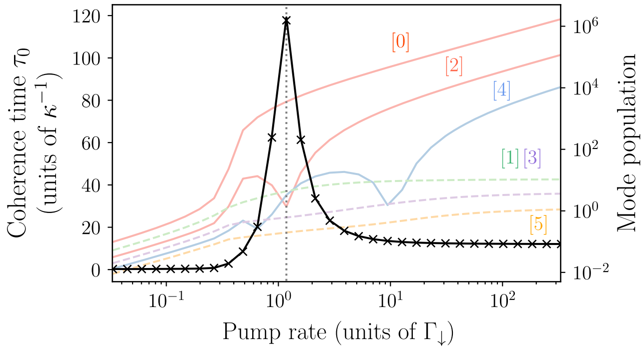

FIG. 1. The breakdown of temporal coherence in photon condensates. The figure shows the ground state coherence time τ_0 as a function of the pump rate $\Gamma_\uparrow$, obtained from Eq. (2) (solid-black line) and via Eq. (5) (black crosses). In the background, the steady state population of the lowest six photon modes ([0,5]) inside the cavity for different pump rates is shown. The coherence of the condensed ground state decreases at the condensation threshold of mode ([2]) (dotted-gray line). For the numerical study, the cavity cutoff (the ground state) frequency is $\omega_0 = 535$ THz, with mode spacing of $\Delta\omega = 1.7$ THz. The photon loss and the molecule decay rate are equal to $\kappa \approx 0.2$ THz and $\Gamma_\downarrow \approx 3 \times 10^{-5}$ THz, respectively. The absorption and emission rates are calculated from experimental data [33].

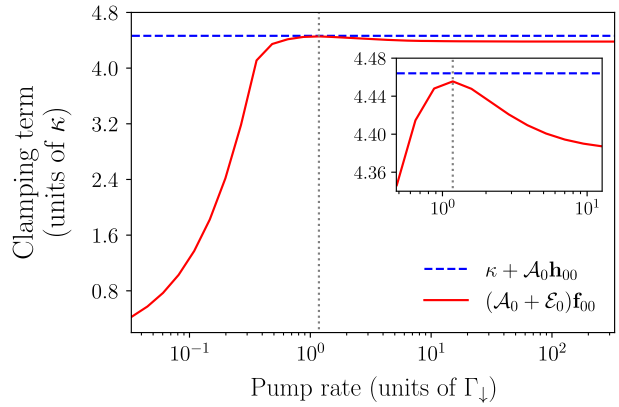

FIG. 2. Variation of the term $(\mathcal{A}_0 + \mathcal{E}_0)\mathbf{f}_{00}$ in Eq. (5) as a function of the pump rate $\Gamma_\uparrow$ (solid-red line), as it converges to $(\kappa + \mathbf{A}_0)\mathbf{h}_0$ (dashed-blue line). The term starts decreasing at the condensation threshold of mode ([2]) (dotted-gray line). Importantly, this decrease is not accompanied by drop in ground state population n_0, as evident from Fig. 1. The inset closes in on the drop of the term around the threshold. The system parameters are the same as Fig. 1.

diagonal. This approximation works well, since Eqs. (3) and (4) involve an integration over the density of dye molecules; for off-diagonal elements, the integrand is oscillatory, whereas it is non-negative for diagonal elements. The integration thus results in a cancellation of terms with different phase for off-diagonal elements in contrast to the accumulation of non-negative contributions for the diagonal terms [34]. Therefore, the solutions of Eq. (2) are expected to behave qualitatively similar to the single-mode case, such that the two-time correlation function reads $c_{pp}(t) = \exp[-t/\tau_p]c_{pp}(0)$ (with $p = 0$ for the ground state), with the coherence time given by

$$\tau_p = \frac{2}{[\kappa + \mathcal{A}_p\mathbf{h}_{pp} - (\mathcal{A}_p + \mathcal{E}_p)\mathbf{f}_{pp}]}. \tag{5}$$

It is instructive to compare this to the steady state population of the ground state

$$n_0 = c_{00}(0) = \frac{\mathcal{E}_0\mathbf{f}_{00} + \sum_{j\neq 0}(\mathcal{E}_j + \mathcal{A}_j)\mathbf{f}_{0j}n_{j0}}{\kappa + \mathcal{A}_0\mathbf{h}_{00} - (\mathcal{A}_0 + \mathcal{E}_0)\mathbf{f}_{00}}, \tag{6}$$

derived from the microscopic model [26] where $n_{j0} = c_{j0}(0)$, is the intermode photon correlation. Since τ_p in Eq. (5) and n_0 in Eq. (6) have the same denominator, one would expect qualitatively similar behavior for the coherence time and the ground state population.

Far below the condensation threshold the molecular excitation at steady state is small. However, as the molecular excitation $\mathbf{f}_{00}$ increases with growing pump power, the term $(\mathcal{A}_0 + \mathcal{E}_0)\mathbf{f}_{00}$ becomes larger, thus lowering the denominator in Eqs. (5) and (6). This leads to an increase of both the photon population n_0 and the coherence time τ_0 of the ground state. The system transitions to the Bose-Einstein condensate phase as the denominator approaches zero, i.e., $\mathbf{f}_{00}$ is clamped to the value $(\kappa + \mathcal{A}_p\mathbf{h}_{pp})/(\mathcal{A}_0 + \mathcal{E}_0)$, and both n_0 and τ_0 diverge. However, if $\mathbf{f}_{00}$ is unclamped due to mode competition and decreases even slightly, the denominator in Eqs. (5) and (6) increases, leading to a loss of coherence time τ_0.

Figure 2 shows the clamping and unclamping of the molecular excitation $\mathbf{f}_{00}$ through the variation of the term $(\mathcal{A}_0 + \mathcal{E}_0)\mathbf{f}_{00}$ with increasing pump power. As the ground state (mode [0]) condenses, the term rapidly approaches its threshold value $(\kappa + \mathcal{A}_0)\mathbf{h}_{00}$. Comparison with Fig. 1 shows that condensation occurs when $\mathbf{f}_{00}$ is clamped to a value close to $(\kappa + \mathcal{A}_0)\mathbf{h}_{00}/(\mathcal{A}_0 + \mathcal{E}_0)$. Notably, Eq. (5) predicts that the coherence time τ_0 rises sharply in this region. In a single-mode system, there is no mechanism that would break this clamping, but unclamping can occur in a multimode system. From Fig. 2, close to the value of $1.18\Gamma_\downarrow$, the excitation profile changes suddenly, i.e., $\mathbf{f}_{00}$ is unclamped due to mode-competition arising from the increase in population of the second-excited state (mode [2]), which leads to a decrease of the coherence time τ_0.

An important question here is why does the ground state population n_0 not decrease along with the coherence time τ_0, when the molecular excitation $\mathbf{f}_{00}$ drops below the threshold. The answer lies in the intermode correlations, which acts to preserve the ground state population, as shown in Eq. (6). In the absence of correlations between the modes (i.e., for $n_{j0} = 0$), the ground state population is given by the contribution $n_e = n_0|_{n_{j0}=0}$, which is driven

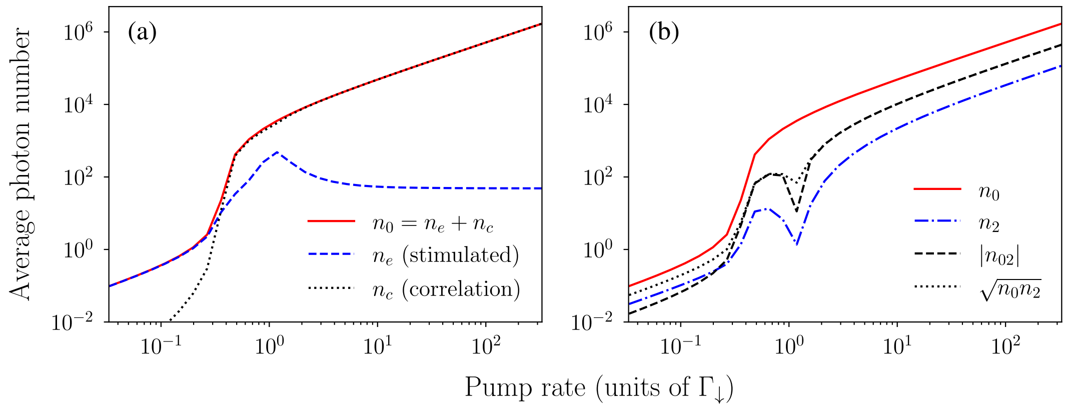

FIG. 3. The contributing terms in the ground state population, the second excited mode and the intermode correlation as a function of rate of pumping. (a) Ground state population, $n_0 = n_e + n_c$ (red, solid), along with the terms arising due to stimulated emission $n_e \propto \mathcal{E}_0 \mathbf{f}_{00}$ (blue, dashed) and intermode correlation $n_c \propto \sum_{j \neq 0} (\mathcal{E}_j + \mathcal{A}_j) \mathbf{f}_{0j} n_{j0}$ (black, dotted). (b) Population of the ground state n_0 (red, solid) and the second-excited mode n_2 (blue, dashed dotted), along with the absolute value of the mode correlation $|n_{02}|$ (black, dashed) and $\sqrt{n_0 n_2}$ (black, dotted). The system parameters are the same as in Fig. 1.

purely by stimulated emission term $\mathcal{E}_0 \mathbf{f}_{00}$. As such, a drop in the molecular excitation $\mathbf{f}_{00}$ would not only result in a decrease of $\mathcal{E}_0 \mathbf{f}_{00}$, but also in an increase of the denominator, $\kappa + \mathcal{A}_0 \mathbf{h}_{00} - (\mathcal{A}_0 + \mathcal{E}_0) \mathbf{f}_{00}$. Hence, for $n_{j0} = 0$ the ground state population n_e decreases along with the coherence time τ_0, whenever $\mathbf{f}_{00}$ is unclamped.

The situation is drastically different in the presence of intermode correlations ($n_{j0} \neq 0$), where any drop in steady state population n_0 due to a decrease in the contribution n_e is countered by an increase in the contribution of $n_c = n_0|_{n_e=0}$. Importantly, n_c is proportional to the mode-correlation dependent term $\sum_{j \neq 0} (\mathcal{E}_j + \mathcal{A}_j) \mathbf{f}_{0j} n_{j0}$ in Eq. (6). Hence, even though the competition for excitation between the modes leads to unclamping of $\mathbf{f}_{00}$ and a decrease in n_e, the correlations between the modes contribute to n_c and compensate for the loss in ground state photons.

Figure 3 shows the behavior of the key terms in the expression for the ground state photon population n_0 [Eq. (6)]. The two main contributing terms, the correlation independent term n_e and the correlation dependent n_c, are shown in Fig. 3(a). The contribution from n_c is substantially larger than that of the correlation independent term n_e. As such, even though the term n_e decreases when $\mathbf{f}_{00}$ is unclamped, the condensed ground state mode population n_0 remains unaffected. However, the condensed mode is no longer temporally coherent as τ_0 decreases with drop in $\mathbf{f}_{00}$. Furthermore, Fig. 3(b), also compares the ground state population n_0 with the second mode population n_2 and the intermode correlation n_{02}. At high pump powers, the correlation n_{02} satisfies the relation $|n_{02}| \simeq \sqrt{n_0 n_2}$. Since the correlation matrix n is positive semidefinite, its elements must satisfy the inequality $|n_{pq}| \leq \sqrt{n_p n_q}$, which implies that the correlation n_{02} is maximal given the mode populations n_0 and n_2. Therefore, even though the off-diagonal excitation matrix element $\mathbf{f}_{02}$ is more than an order of magnitude smaller than the diagonal term $\mathbf{f}_{00}$ (with $|\mathbf{f}_{02}/\mathbf{f}_{00}| \approx 10^{-2} - 10^{-4}$), the large value of n_{20} ensures that the correlation dependent term n_c in Eq. (6) is large enough to ensure that the ground state photon number n_0 remains unchanged.

Another question is whether the condensing mode is a superposition of several modes. Diagonalizing the correlation matrix $n_{ij} = c_{ij}(0)$ shows that the proportion of the photons in the ground state p_0 is rather high ($p_0 \geq 0.93$), compared to modes [2] ($p_2 \leq 0.064$) and mode [4] ($p_4 \leq 6 \times 10^{-3}$), and the average population of the odd modes are negligible. Another interesting observation in Fig. 1 is that only the even modes ([0],[2],[4]) condense, whereas the odd modes ([1],[3],[5]) are poorly populated. The spatial profile of the pump is not uniform in the cavity, but rather a Gaussian of finite width focused at the center. As such, even modes, with mode functions that peak at the center, have greater access to excited molecules and also correlate more strongly with the ground state. This behavior is nullified by moving the pump spot.

The intermode correlations also give rise to other effects. For instance, the population n_2 of the second-excited mode increases when the ground state mode condenses, for pump rate values between $0.2\Gamma_\downarrow$ and $0.5\Gamma_\downarrow$, as shown in Figs. 1 and 3(b). The explanation lies in the intermode correlation between the ground and second excited mode, which is anti-correlated ($n_{20} < 0$) at low pump powers. However, in this regime the off-diagonal excitation term $\mathbf{f}_{20}$ is also negative, which leads to a net positive contribution to the population, as shown by the absolute value of n_{20} in Fig. 3(b). This rise in n_2 is purely driven by the correlations, as the contribution due to stimulated emission $\mathcal{E}_2 \mathbf{f}_{22}$ remains significantly smaller. Another interesting observation is that the temporal coherence does not completely disappear at higher pump powers in

Fig. 1. This is due to the fact that the number of photons arising from stimulated emission n_e does not vanish but converges to a significant steady state value at high pump powers, as shown in Fig. 3.

The presently used nonequilibrium model for photon condensation [26] provides the footing to identify intermode correlations as the cause for changes in molecular excitation profile, which ultimately leads to the breakdown of temporal coherence, thus contradicting the behavior predicted by the Schawlow-Townes limit. The mechanism studied here is quite general and similar effects of intermode correlations could be engineered in other optical systems, where it could lead to generation of partially coherent light, which is a powerful resource in imaging [35] and communications [36]. A future direction is to investigate temporal coherence during other nonequilibrium phenomena such as decondensation, where a higher mode forces a lower condensed mode to lose its population. In such a regime, the simultaneous loss of temporal coherence and decondensation in a pair of higher energy modes, could lead to favorable changes in the molecular excitation profile and recoherence in the ground state mode. Other avenues include the study of quantum correlations developing between coupled, but spatially separated modes [37], especially in condensates with only a few photons. These will prove useful in manipulation of quantum states of light [38], with potential application in interferometry and metrology.

The authors acknowledge financial support from the European Commission via the PhoQuS Project (H2020-FETFLAG-2018-03) No. 820392 and the EPSRC (U.K.) through Grant No. EP/S000755/1. H. S. D. acknowledges financial support from SERB-DST, India via a Core Research Grant CRG/2021/008918 and the Industrial Research & Consultancy Centre, IIT Bombay via Grant (RD/0521-IRCCSH0-001) No. 2021289.

[1] D. P. DiVincenzo and D. Loss, Quantum computers and quantum coherence, J. Magn. Magn. Mater. **200**, 202 (1999).

[2] Y. Wu, Q. Wu, F. Sun, C. Cheng, S. Meng, and J. Zhao, Emergence of electron coherence and two-color all-optical switching in MoS_2 based on spatial self-phase modulation, Proc. Natl. Acad. Sci. U.S.A. **112**, 11800 (2015).

[3] E. Rodriguez, N. George, J.-P Lachaux, J. Martinerie, B. Renault, and F. J. Varela, Perception's shadow: Long-distance synchronization of human brain activity, Nature (London) **397**, 430 (1999).

[4] L. Mandel and E. Wolf, *Optical Coherence and Quantum Optics* (Cambridge University Press, Cambridge, Cambridge, England, 1995).

[5] W. Ketterle, Nobel lecture: When atoms behave as waves: Bose-Einstein condensation and the atom laser, Rev. Mod. Phys. **74**, 1131 (2002).

[6] J. Kasprzak, M. Richard, S. Kundermann, A. Baas, P. Jeambrun, J. M. J. Keeling, F. M. Marchetti, M. H. Szymańska, R. André, J. L. Staehli, V. Savona, P. B. Littlewood, B. Deveaud, and Le Si Dang, Bose-Einstein condensation of exciton polaritons, Nature (London) **443**, 409 (2006).

[7] J. Klaers, J. Schmitt, F. Vewinger, and M. Weitz, Bose-Einstein condensation of photons in an optical microcavity, Nature (London) **468**, 545 (2010).

[8] J. Marelic and R. A. Nyman, Experimental evidence for inhomogeneous pumping and energy-dependent effects in photon Bose-Einstein condensation, Phys. Rev. A **91**, 033813 (2015).

[9] T. K. Hakala, A. J. Moilanen, A. I. Väkeväinen, R. Guo, J.-P. Martikainen, K. S. Daskalakis, H. T. Rekola, A. Julku, and P. Törmä, Bose-Einstein condensation in a plasmonic lattice, Nat. Phys. **14**, 739 (2018).

[10] S. Barland, P. Azam, G. L. Lippi, R. A. Nyman, and R. Kaiser, Photon thermalization and a condensation phase transition in an electrically pumped semiconductor microresonator, Opt. Express **29**, 8368 (2021).

[11] J. Bloch, I. Carusotto, and M. Wouters, Non-equilibrium Bose-Einstein condensation in photonic systems, Nat. Rev. Phys. **4**, 470 (2022).

[12] B. T. Walker, L. C. Flatten, H. J. Hesten, F. Mintert, D. Hunger, A. A. P. Trichet, J. M. Smith, and R. A. Nyman, Driven-dissipative non-equilibrium Bose-Einstein condensation of less than ten photons, Nat. Phys. **14**, 1173 (2018).

[13] H. S. Dhar, Z. Zuo, J. D. Rodrigues, R. A. Nyman, and F. Mintert, Quest for vortices in photon condensates, Phys. Rev. A **104**, L031505 (2021).

[14] B. T. Walker, H. J. Hester, H. S. Dhar, R. A. Nyman, and F. Mintert, Noncritical slowing down of photonic condensation, Phys. Rev. Lett. **123**, 203602 (2019).

[15] J. Schmitt, T. Damm, D. Dung, F. Vewinger, J. Klaers, and M. Weitz, Observation of grand-canonical number statistics in a photon Bose-Einstein condensate, Phys. Rev. Lett. **112**, 030401 (2014).

[16] B. T. Walker, J. D. Rodrigues, H. S. Dhar, R. F. Oulton, F. Mintert, and R. A. Nyman, Non-stationary statistics and formation jitter in transient photon condensation, Nat. Commun. **11**, 1390 (2020).

[17] D. Sanvitto, F. M. Marchetti, M. H. Szymanska, G. Tosi, M. Baudisch, F. P. Laussy, D. N. Krizhanovskii, M. S. Skolnick, L. Marrucci, A. Lemaitre, J. Bloch, C. Tejedor, and L. Vina, Persistent currents and quantized vortices in a polariton superfluid, Nat. Phys. **6**, 527 (2010).

[18] I. Amelio and I. Carusotto, Theory of the coherence of topological lasers, Phys. Rev. X **10**, 041060 (2020).

[19] J. Klaers, F. Vewinger, and M. Weitz, Thermalization of a two-dimensional photonic gas in a "white wall" photon box, Nat. Phys. **6**, 512 (2010).

[20] R. A. Nyman and M. H. Szymańska, Interactions in dye-microcavity photon condensates and the prospects for their observation, Phys. Rev. A **89**, 033844 (2014).

[21] D. W. Snoke and S. M. Girvin, Dynamics of phase coherence onset in Bose condensates of photons by incoherent phonon emission, J. Low Temp. Phys. **171**, 1 (2013).

[22] J. Marelic, L. F. Zajiczek, H. J. Hesten, K. H. Leung, E. Y. X. Ong, F. Mintert, and R. A. Nyman, Spatiotemporal

coherence of non-equilibrium multimode photon condensates, New J. Phys. **18**, 103012 (2016).

[23] T. Damm, D. Dung, F. Vewinger, M. Weitz, and J. Schmitt, First-order spatial coherence measurements in a thermalized two-dimensional photonic quantum gas, Nat. Commun. **8**, 158 (2017).

[24] A. L. Schawlow and C. H. Townes, Infrared and optical masers, Phys. Rev. **112**, 1940 (1958).

[25] P. Kirton and J. Keeling, Thermalization and breakdown of thermalization in photon condensates, Phys. Rev. A **91**, 033826 (2015).

[26] Y. Tang, H. S. Dhar, R. F. Oulton, R. A. Nyman, and F. Mintert, companion paper, Photon-photon correlation of condensed light in a microcavity, Phys. Rev. A **109**, 043713 (2024).

[27] H. J. Hesten, R. A. Nyman, and F. Mintert, Decondensation in nonequilibrium photonic condensates: When less is more, Phys. Rev. Lett. **120**, 040601 (2018).

[28] C. H. Henry, Theory of the linewidth of semiconductor lasers, IEEE J. Quantum Electron. **18**, 259 (1982).

[29] J. Klaers, J. Schmitt, T. Damm, F. Vewinger, and M. Weitz, Bose-Einstein condensation of paraxial light, Appl. Phys. B **105**, 17 (2011).

[30] H. Alaeian, M. Schedensack, C. Bartels, D. Peterseim, and M. Weitz, Thermo-optical interactions in a dye-microcavity photon Bose-Einstein condensate, New J. Phys. **19**, 115009 (2017).

[31] J. Keeling and P. Kirton, Spatial dynamics, thermalization, and gain clamping in a photon condensate, Phys. Rev. A **93**, 013829 (2016).

[32] P. Kirton and J. Keeling, Nonequilibrium model of photon condensation, Phys. Rev. Lett. **111**, 100404 (2013).

[33] R. A. Nyman (2017), 10.5281/zenodo.569817.

[34] The approximation made while solving Eq. (2) has been verified numerically, where the contributions of the off-diagonal terms in estimating the coherence time is found to be negligible compared to the diagonal terms.

[35] M. Singh, H. Lajunen, J. Tervo, and J. Turunen, Imaging with partially coherent light: Elementary-field approach, Opt. Express **23**, 28132 (2015).

[36] Y. Huang *et al.*, Optical broadcasting employing incoherent and low-coherence spatial modes for bi-directional optical wireless communications, J. Lightwave Technol. **39**, 833 (2021).

[37] C. Kurtscheid, D. Dung, E. Busley, F. Vewinger, A. Rosch, and M. Weitz, Thermally condensing photons into a coherently split state of light, Science **15**, 894 (2019).

[38] M. Vretenar, C. Toebes, and J. Klaers, Modified Bose-Einstein condensation in an optical quantum gas, Nat. Commun. **12**, 5749 (2021).